JOURNAL OF MATERIALS SCIENCE **36** (2001) 3071 – 3077

Studies of the mesophase development in polymeric fibers during deformation by synchrotron SAXS/WAXD

SHAOFENG RAN, XINHUA ZONG, DUFEI FANG,
BENJAMIN S. HSIAO, BENJAMIN CHU*
Department of Chemistry, State University of New York at Stony Brook, Stony Brook, New York, 11794-3400, USA
E-mail: Bchu@notes.cc.sunysb.edu

P. M. CUNNIFF
US Army Soldier and Biological Chemical Command, Natick, MA 01760-5019, USA

R. A. PHILLIPS
Montell Polyolefins. R&D Center, 912 Appleton Road, Elkton, MD 21921, USA

On-line structural and morphological studies on Kevlar 49 and isotactic polypropylene (iPP) fibers during deformation were carried out using synchrotron small-angle X-ray scattering (SAXS) and wide-angle X-ray diffraction (WAXD). A novel image analysis method was used to extract quantitative fractions of the crystal phase, the amorphous phase and a "mesomorphic" (intermediate) phase from two-dimensional (2D) WAXD patterns. Results showed that about 20 wt% in the Kevlar 49 fiber had an intermediate mesophase morphology. The transitions between crystal phase, amorphous phase and mesophase were not obvious during deformation of Kevlar 49 fiber at room temperatures. 2D SAXS patterns indicated that the superstructure of the Kevlar 49 fiber was fibril in nature. 2D WAXD results of iPP fibers showed that the α-form crystals were quite defective in the initial state and were converted to the well-known mesomorphic form by drawing at room temperatures. The mesophase in Kevlar 49 fibers was then compared with that in iPP fibers. The shape of one-dimensional equatorial peak of the mesophase in the iPP fiber was similar to that in the Kevlar fiber, indicating that the mesophase in both iPP and Kevlar fibers could be similar in some aspects of molecular arrangement. Corresponding 2D SAXS patterns showed that there was no obvious long period in the mesophase of the drawn iPP fiber. We speculate that the constituents of the mesomorphic fraction extracted in the drawn iPP fibers may consist of partially oriented bundles of helical chains with random helical hands as well as oriented chains with no helical structures (consisting of stereo/tacticity defects). The latter is similar to the mesophase of rigid chains in Kevlar fibers, consisting of only oriented chains with no helical structures.

1. Introduction

Recent experimental findings [1–3] indicate that the structure of polymeric fiber should include an intermediate phase between crystalline and amorphous fractions, which may be due to the one- or two-dimensional ordering of polymer chains in the drawn fibers. The intermediate phase (mesophase) represents a state of order between the zero long-range ordering (amorphous state) and the three-dimensional (3D) crystalline ordering.

The mesophase has been reported in many polymers, such as polypropylene [4–7], polyethylene [1, 3] and PET [3]. Natta first reported the mesophase in isotactic polypropylene (iPP) in 1959 [4]. Since then, many comprehensive studies on the mesophase of iPP have been carried out. However, there are still arguments on the nature of the mesophase. Bruckner *et al*. [5] pointed out that the statistical structure of mesomorphic iPP eliminated the possibility that the mesomorphic form might consist of small crystals of the α form or the β form. Wunderlich and Grebowicz [8, 9] proposed that the concept of conformationally disordered crystal could be used to explain the mesomorphic form. Corradini *et al*. [6, 10] concluded that the mesophase of iPP was not composed of small pseudohexagonal crystals, but of much more disordered bundles of chains.

* Author to whom all correspondence should be addressed.

Kevlar aramid fiber, having a chemical structure of poly(*p*-phenylene terephthalamide), is a high-performance fiber that possesses high tensile modulus, tensile strength and thermal stability [11]. Although the mesophase in Kevlar fibers had not yet been fully discussed, Dobb *et al*. [12] stated that there was evidence for the existence of two-dimensional ordering in Kevlar fibers based on the layer-like streaking in electron diffraction patterns. The results of ^{2}H NMR spectroscopy indicated that the dynamics were quite heterogeneous in structure. Thus, a less perfectly ordered structure could exist, probably from chains residing at or close to the crystallite surface [13–16].

Of course, the major difference between iPP and aramid fibers is the basic building block. The aramid chain is rigid and mesogenic which does not have any optical chirality, but can be aligned easily to form a liquid crystallite. In contrast, iPP is a chiral polymer, which can possess different helical hands: right-handed or left-handed (3_1 and 3_2 helices). The mesomorphic phase in iPP (some groups have identified it as smectic [4]) is thought to have a parallel assembly of helical chains, in which the helical hand is random. It is also conceivable that the iPP chains can be oriented having no helical structure, probably due to the stereo or tacticity defects.

It is generally difficult to investigate the mesophase because there is no straightforward method that is able to extract the fraction of the mesophase quantitatively. In this study, we introduce an integrative X-ray diffraction image analysis method that is capable of extracting the quantitative fraction of the mesophase, although we cannot differentiate the type of mesophase or determine its location in the internal structure. The transitions between the crystal phase, the mesophase and the amorphous phase were then studied during the fiber deformation.

The mesophase extracted in this study represents the mass fraction of intermediate phase(s) between the amorphous phase and the ordered crystalline phase. For the case of iPP, the mesophase mentioned by Natta [4], Bruckner [5], Wunderlich [8], Grebowicz [9] and Corradini *et al*. [6, 10] is often considered as the smectic phase, or even "mesomorphic" crystallites [7]. The mesomorphic content extracted in this work will include this contribution. In addition, it may also include the bundle-like aggregate of chains with helical structures (randomly oriented hands) or without helical structure (like oriented amorphous chains).

2. Experimental

Two different kinds of fibers were studied. One was the commercial Kevlar 49 fiber. The other was the iPP fiber provided by the Montell USA Company. The iPP resin was a commercial Ziegler-Natta resin (Montell PF-304) with M_w of $\sim 1.8 \times 10^5$ g/mol, M_w/M_n of ~ 3 and melt flow rate index of 40 g/10 min. The iPP fibers were spun on a Hills Model REM-3MP-25 spinning unit with temperature of 216 °C at a take-up velocity of 1000 m/min into a 41 filament yarn with ~ 5 denier/filament. The spun fibers were quenched at air temperature of 13 °C. Synchrotron X-ray measurements were carried out at the State University of New York (SUNY) X27C beam line, the National Synchrotron Light Source (NSLS), Brookhaven National Laboratory (BNL). The wavelength was 1.307 Å. The beam size was 0.6 mm in diameter by using a 3-pinhole collimator system [17, 18]. The 2D WAXD patterns were recorded by a MAR CCD x-ray detector (MARUSA) for quantitative image analysis. Separate simultaneous SAXS and WAXD patterns were recorded using Fuji^{TM} HR-V imaging plates which were then digitized using a Fuji^{TM} BAS 2000 IP imaging plate scanner. The WAXD imaging plate images were used to compare with the CCD images. The collection time for both WAXD and SAXS measurements was 2 min. Kevlar 49 and iPP fibers were both drawn at room temperatures.

For Kevlar 49 fiber, a stretching unit was used because the Kevlar 49 fiber had a typical draw-to-break ratio of only about 3.0% [11]. The stretching unit was a modified Instron model 4410 apparatus. The modification allowed symmetrical stretching of the sample, in order to assure that the focused X-rays always illuminated the same position on the fiber during deformation. The chosen stretching speed was 3 mm/min using an initial fiber length of 30.0 mm. After having reached the desired stretch ratio, the fiber was held for 2 min for image collection and was then subjected to the next stretch ratio. For SAXS measurements, the fiber was held for 5 more minutes allowing the image to be digitized. The distance between the sample and the detector for WAXD was 90.7 mm, and for SAXS was 1156.0 mm.

For the iPP fiber, a continuous fiber draw apparatus was used (Fig. 1). This industrial prototype draw apparatus was originally designed by A. D. Kennedy (DuPont), modified by us and constructed by Hills Inc. (W. Melbourne, Florida). The feeding speed was kept at 4 m/min during the experiment, while the drawing speed was continuously adjusted to achieve the desired draw ratio. The sample to detector distance for WAXD measurements with the CCD detector was 114.5 mm and for SAXS was 1138.0 mm.

The elimination of air scattering was important for detailed data analysis. Thus, a PIN-diode beam stop was used in the experiment in order to make an accurate

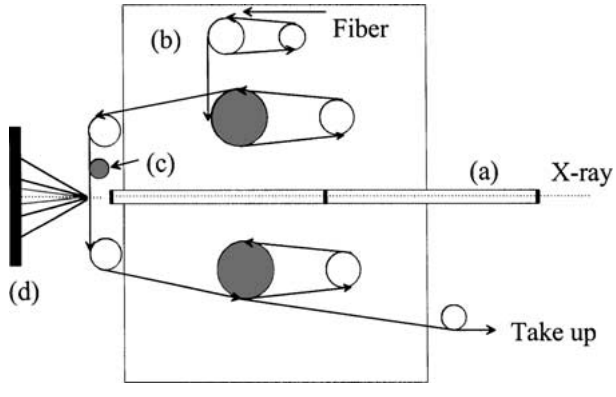

Figure 1 Schematic diagram of the continuous draw apparatus for the on-line WAXD/SAXS measurement. (a) three-pinhole collimator; (b) draw apparatus with continuous feed yarn; (c) hot-pins; (d) WAXD/SAXS detector.

correction of air scattering. The PIN-diode used was a silicon-based photo-diode with a diameter of 3.0 mm. The PIN-diode recorded the transmitted intensity after the incident X-ray beam passed through the fiber and could be used to estimate the effect of sample absorption. The details for the background correction with the PIN-diode beam stop has been reported elsewhere [19].

3. Results and discussion

Fig. 2 illustrates the 2D WAXD pattern of the Kevlar fiber at a stretch ratio of 3.0% at room temperature. This pattern has been corrected for the incident beam fluctuations and air scattering. Two strong equatorial reflections, indexed as (110) and (200), show a narrow spread along the azimuthal direction, indicating that the Kevlar fiber has a high degree of crystal orientation along the fiber axis. The successive layer lines are associated with the molecular repeat spacing of the Kevlar molecules stacked in the meridional direction.

In order to deconvolute the crystal, mesomorphic and amorphous fractions, a new method was used to analyze the WAXD patterns. The 2D WAXD pattern after correction of air scattering and incident X-ray beam fluctuations can be considered as a combination of two components: an isotropic part and an anisotropic part. The isotropic scattering represents unoriented structures in the fiber, which is independent of the azimuthal angle. More specifically, the isotropic scattering includes the scattering from the unoriented amorphous phase and the Compton scattering from the chemical structure which is usually small at typical detection angular range and can be ignored. The isotropic fraction $A_{\mathrm{iso}}(s)$ can be extracted by using the "*Halo*" method described below.

Starting from the center of the scattering pattern, a series of azimuthal scans can be obtained as a function of s ($[=2\sin(\theta/2)/\lambda]$ is the scattering vector and θ is the scattering angle). All of the minimum intensities of the sequential azimuthal scans thus represent the envelope of the isotropic contribution.

The anisotropic fraction $A_{\mathrm{an}}(s,\phi)$ then can be calculated from the following equation:

$$A_{\mathrm{an}}(s,\phi) = A(s,\phi) - A_{\mathrm{iso}}(s) \qquad (1)$$

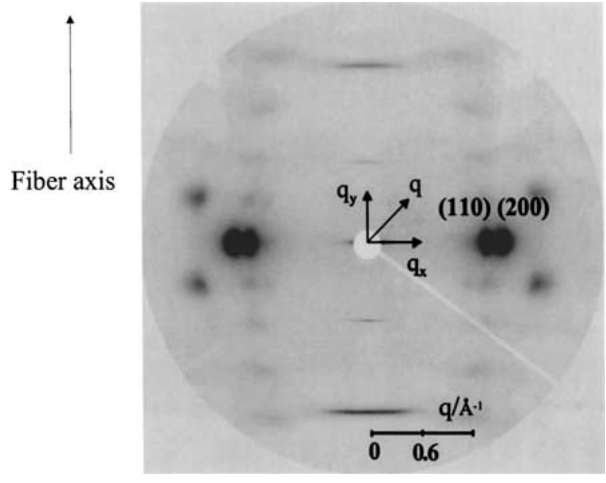

Figure 2 2D WAXD pattern of Kevlar 49 fiber at a stretch ratio of 3.0% at room temperature.

where $A(s,\phi)$ is the total scattering and ϕ is the azimuthal angle. The anisotropic scattering represents the oriented structures in the fiber, including both the crystal phase and the mesophase. A two-dimensional (2D) peak fit routine was used to separate the crystal phase and the mesophase in the anisotropic fraction of the scattering. By considering the mesophase to represent the highly oriented fraction of the chains with poor intermolecular ordering when compared with the packing in crystals, most of the scattered intensity contributed by the mesophase is expected to appear on the equator. The intensity of the scattering on the layer line was relatively weak. As a result, in the 2D deconvolution procedure, we first selected a region along the equatorial direction which contained the main crystal reflections (such as (110) and (200) in Kevlar 49) and the oriented diffused scattering background. By assuming that both the crystal phase and the mesophase could be described as 2D Gaussian functions (Eq. 2) then the crystal reflections and the mesophase (diffused scattering background) could be numerically separated.

$$f = h\,\exp\left(-\left(\frac{s_{x0}-s_x}{\omega_x}\right)^2 - \left(\frac{s_{y0}-s_y}{\omega_y}\right)^2\right) \qquad (2)$$

where the subscript "0" represents the peak position, ω is the full width at half maximum, h represents the height of the peak, s is the scattering vector and s_x, s_y are the scattering vector values in the Cartesian coordinate of the reciprocal space ($\mathrm{s}_x = 2\sin(\theta_x/2)/\lambda$). Fig. 3 shows the WAXD pattern of Kevlar 49 before the 2D peak fit (anisotropic scattering) and the 2D as well as 1D patterns of the crystal phase and the mesophase deconvoluted by the 2D peak fit method. The mesophase peak of Kevlar fiber was broad, indicating that the mesophase determined in such a fashion was quite disordered. In contrast, the crystal phase had a regular three-dimensional order, which formed sharp reflection peaks. The areas of the crystal and the mesomorphic reflections calculated by the 2D peak fit could be used to estimate the fractions of the two different phases. The percentage of the residues in the 2D peak fit procedure was about 2%.

Fig. 4 shows the variation of the crystal, mesomorphic and amorphous mass fractions of Kevlar 49 fiber calculated by the above method at different stretch ratios. The mesophase percentage in the Kevlar 49 fiber was around 20–25% (by weight), suggesting that about 20% of the chains could be considered in the intermediate state between the crystalline and the amorphous phases. However, from the X-ray investigation, we still do not know exactly the location of the mesophase in the fiber. In view of the reported morphology and crystallinity in the Kevlar fiber thus far [12–16], we speculate that the mesophase could represent the highly oriented fraction of the chains with lattice registrations too low to be considered as crystalline. The loss of the lattice registrations may occur due to occasional defects in the crystal packing, a common feature in fibers, since the fiber processing usually involves structural formation under tension. Another possibility is that the well-defined crystals may lose one or two-dimensional order(s) during deformation, thereby forming the

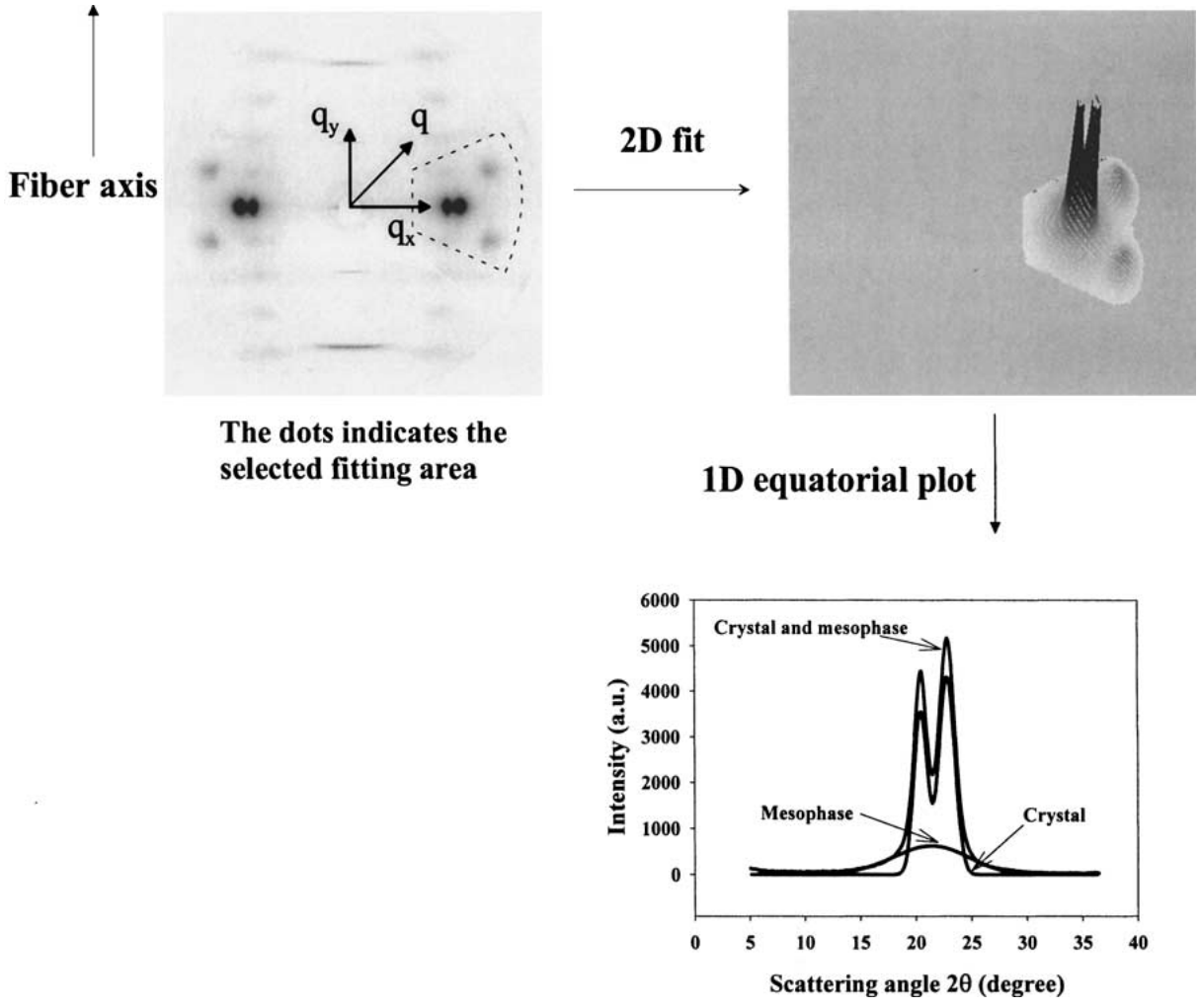

Figure 3 WAXD pattern of Kevlar 49 at a stretch ratio of 3.0% before 2D peak fit and the 2D/1D patterns of the crystal phase and the mesophase extracted by the 2D peak fit method.

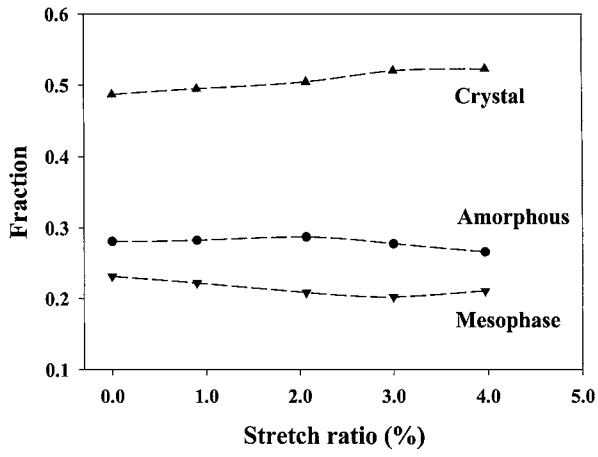

Figure 4 Variation of crystal, mesomorphic and amorphous fractions of Kevlar 49 fiber as a function of stretch ratio at room temperature.

mesophase. The chains in the mesophase have only partial ordering and pack nonregularly along the fiber axis. Such a molecular arrangement in the mesophase may result in higher tenacity and a higher ability for the fibers to elongate than the fibers with only the crystal fraction. Thus, the mesophase could be a possible route that may provide us with a desirable pathway to develop high performance fibers with higher tenacity. The amorphous fraction is near 30%, which is slightly higher than the mesophase. The amorphous phase of the Kevlar fiber could be located on the boundary of the crystals or the fibril interfaces. The amorphous fraction may also correspond to the defect layer proposed by Panar *et al*. and Pruneda *et al*. [20–21]. The percentage of 30 wt% is quite similar to the estimation made by English *et al*. [13–16], who pointed out that about 40% of the chains in Kevlar fibers resided on the surface of the crystals since the crystal size was quite small. The unoriented chains on the crystal surface could result in an amorphous structure.

It is noted that the changes in the fractions of the amorphous, crystal and mesomorphic phases during stretching are not obvious because the stretch ratios are small and the deformation takes place at room temperatures. However, there is evidence indicating that the conversion between crystal, amorphous and mesomorphic phases is real. The crystallinity was found to increase slightly with increasing stretch ratio. The fraction of the mesophase decreased and the fraction of the amorphous phase did not change much before the stretch ratio reached 3.0%, indicating that the mesophase might be converted to the crystal phase. These results implied that the mesophase was a metastable phase. We believe that stretching could

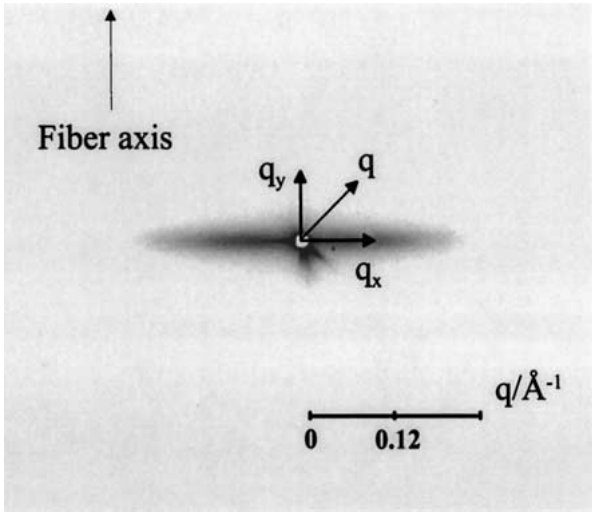

Figure 5 2D SAXS pattern of Kevlar 49 fiber with stretch ratio of 3.0% at room temperature.

provide the kinetic energy that facilitates the lateral registration forming a three-dimensional crystal structure. Above the stretch ratio of 3.0%, it was found that the fraction of the mesophase increased and that of the amorphous phase decreased, since the chains in the amorphous phase could be oriented at high stretch ratios and packed with some kind of ordering to form the mesophase.

Fig. 5 shows the 2D SAXS pattern of Kevlar 49 fiber at the stretch ratio of 3.0%. The SAXS pattern has a streak along the equatorial direction. However, there is no apparent scattering along the meridian. The streak pattern indicates that the Kevlar 49 fiber has mainly a fibrillar superstructure, with no trace of lamellar morphology. Grubb *et al*. also did not observe any evidence of lamellar structure in Kevlar 49 and Kevlar 149 fiber in their work [22], which is consistent with our result.

The interpretation of the equatorial streak in SAXS is more complicated, since it may contain several contributions including the microfibrillar structure, voids morphology and the surface reflection/scattering of the fiber. Previous studies [22] pointed out that the scattering objects in Kevlar 49 were mainly associated with the microfibrillar structure, not from the void morphology. We agree with this conclusion. Scattering objects extended along the fiber direction produce the streak on the equator. If the objects are perfectly aligned in the fiber direction and have a finite length, then the angular width of the streak should be constant. However, in most cases, both the size distribution and the misorientation of the scattering object have contributed to the streak profile.

We cannot identify the exact location and the composition of the mesophase only from the WAXD/SAXS results because we do not have Kevlar samples with only the mesophase. Thus, the 2D WAXD patterns of iPP fibers were analyzed in order to compare with the results from Kevlar fibers.

Fig. 6 illustrates the 2D WAXD patterns of iPP fiber with different draw ratios at room temperatures. These WAXD patterns have been corrected for beam fluctuations and air scattering. Fig. 6a is the pattern of the original fiber before drawing, indicating that the initial fiber is only partially oriented. The three strong peaks located on the equator had the characteristics of the α form of polypropylene crystal, which could be indexed as the (110), (040) and (130) reflections, respectively. The three peaks were slightly superposed in the initial fiber. One possible reason is that the crystals in the initial iPP fiber might be defective. The other is the possible presence of the mesomorphic form mixed with the α-crystal form in the original fiber. As the crystal density is often used to evaluate the perfection of the crystals, we have calculated the crystal densities from the unit cell parameters. The method used to calculate the unit cell parameters from WAXD pattern has been reported previously [23]. We found that the calculated crystal density was 0.90 g/cm^3 from the initial fiber, which was much lower than the ideal α-form crystal density (0.936 g/cm^3) and only slightly greater than the density of the mesophase (0.88 g/cm^3) measured by Natta *et al*. [4], implying that the α-form crystallites were quite defective and could be mixed with the mesomorphic crystallites in the initial fiber.

With increasing draw ratio, the azimuthal spread of the reflections became narrower in Fig. 6, indicating that the crystal orientation increased with increasing draw ratio. It is interesting to note that the superposition of the three α-form equatorial peaks also becomes more severe, indicating the fraction of the intermediate phase(s) has increased. At a draw ratio of 2.5, the three equatorial peaks completely disappear, resulting in one broad peak. This broad equatorial peak and the four

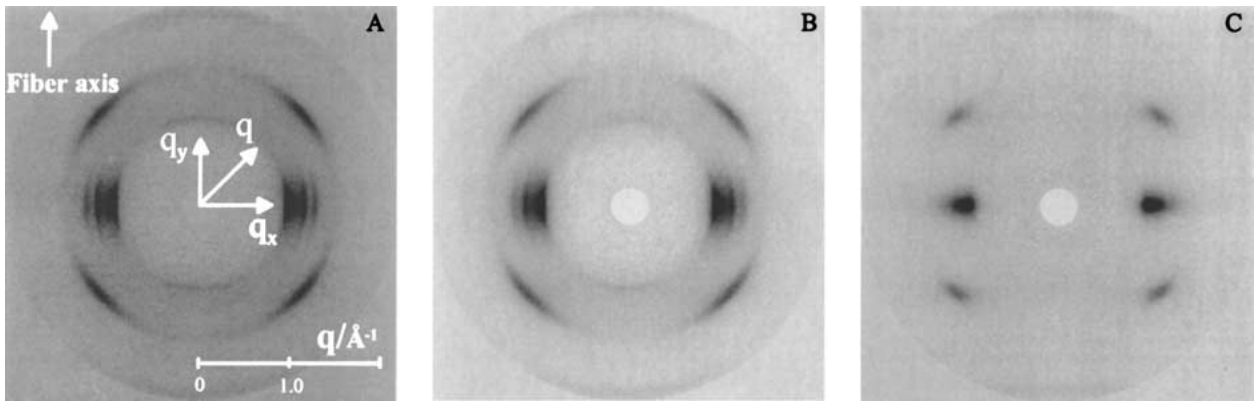

Figure 6 2D WAXD patterns of iPP fiber with different draw ratios at room temperature. Draw ratio: A: 1.0, B: 1.5, C: 2.5.

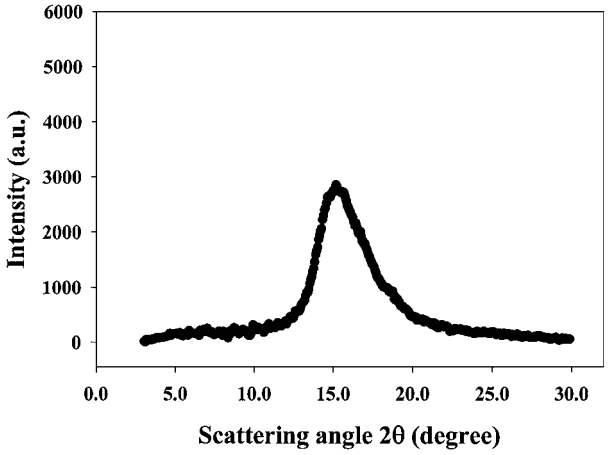

Figure 7 One-dimensional equatorial plot of the mesophase in iPP fiber at a draw ratio of 2.5.

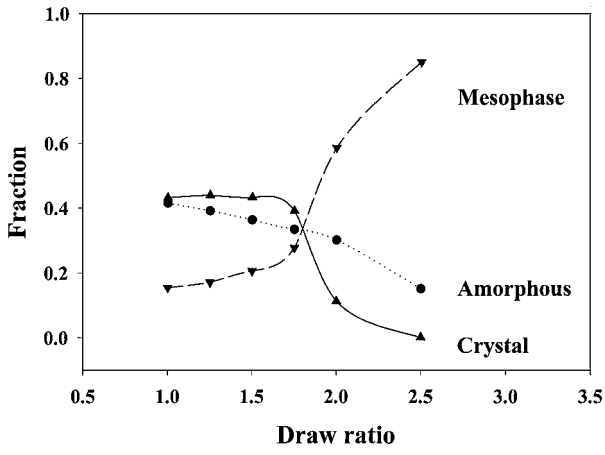

Figure 8 Fraction of crystal, mesomorphic and amorphous phases of iPP fiber as a function of draw ratio at room temperature.

off-axis peaks (at the first layer line) are often regarded as the WAXD fingerprint of the mesomorphic form in iPP [24–25]. Fig. 7 shows the one-dimensional equatorial plot of the mesophase in iPP (Fig. 6c). Compared with Fig. 3, it is found that the 1D equatorial plots of the mesophase in both iPP and Kevlar 49 fibers show a very similar broad peak, although the peak position is different. This observation suggests that the two mesophases in Kevlar 49 and iPP fibers may be similar in nature. Thus, it is reasonable to conclude that the mesophase fraction in Kevlar 49 fibers is real. The 2D WAXD patterns in Fig. 6 imply that the α-form crystals in the iPP fibers could be converted into the mesomorphic form by drawing at room temperature [26]. The four distinct peaks on the first layer line are due to the helical chain structure (3_1 or 3_2). This result indicates that the mesophase of iPP fiber maintains the helical chain conformation, which has been confirmed by many earlier studies [26–29]. The helical chain structure does not exist in the amorphous phase, because there is no ordering in the amorphous phase, which is one of the differences between the mesophase and the amorphous phase in iPP fibers.

Fig. 8 shows the variations of the crystal, mesomorphic and amorphous fractions of iPP fibers with different draw ratios at room temperatures. At low draw ratios (<1.5), the crystal fraction remained about constant, while the mesophase increased and the amorphous fraction decreased slightly. Above a draw ratio of 1.5, the mesomorphic fraction increased dramatically. The corresponding crystal fraction and the amorphous phase all decreased, but a steeper decline was seen in the crystal phase. Our explanation is that the molecular mobility of the polymer chains is quite low at room temperatures, such that crystallization induced by drawing is not feasible. At low draw ratios, the energy provided by drawing is not sufficient to deform the crystal structure even if the crystals were defective. However, the chains in the amorphous phase could be oriented into the ordered state, which constitutes the mesophase. When the draw ratio becomes so large that drawing can destroy the lateral registrations of the chains in the defective crystals, the crystal phase has been converted to the mesophase. With the addition of the mesophase converted from the amorphous chains, the total fraction of the mesophase increases quickly with the draw ratio.

Fig. 9 shows the corresponding 2D SAXS patterns of the iPP fiber as a function of draw ratio at room temperatures. Fig. 9a is the pattern of the iPP fiber before drawing, which exhibits a two-bar pattern with the scattering maxima on the meridional direction. This feature indicates the existence of the lamellar structure in the fiber. With increasing draw ratio, the two-bar pattern became smeared, with the peak position shifting toward a lower value (the lone period becomes larger), suggesting the destruction and the deformation of the lamellar

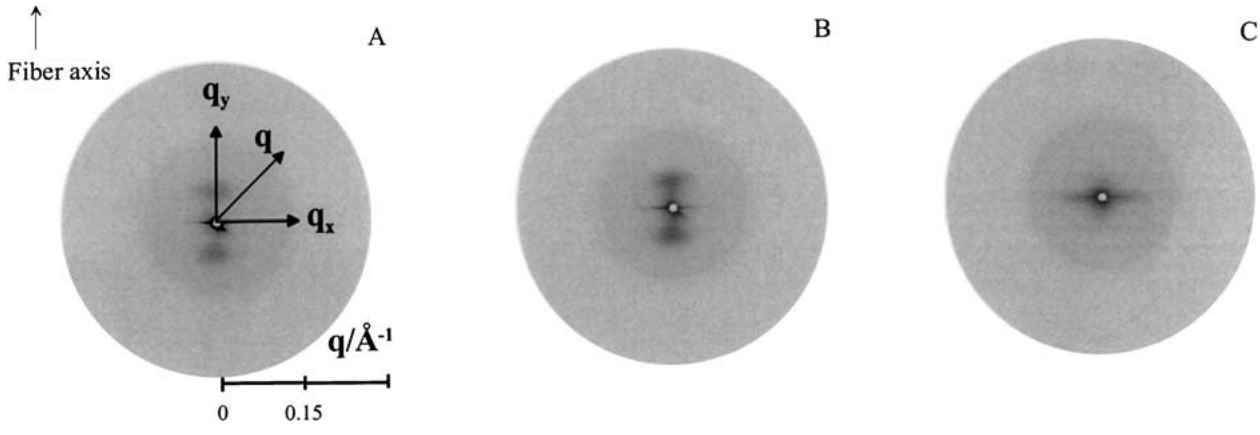

Figure 9 2D SAXS patterns of iPP fiber with different draw ratios at room temperature. Draw ratio: A: 1.0, B: 1.5, C: 2.5.

structure. When the draw ratio reached 2.5, the scattering maxima on the meridian disappeared (Fig. 9c), resulting in a dominant streak pattern on the equator. The result suggests that the well-defined lamellar structure containing alternative crystalline and amorphous phases in the iPP fibers could probably be destroyed to form a more disordered structure with highly oriented chains. The WAXD result in Fig. 6c showed that the SAXS pattern of Fig. 9c was almost totally mesomorphic, suggesting that the dominant mesophase formed in the drawn iPP fiber exhibit a SAXS pattern quite similar to that of Kevlar fiber (Fig. 5). Thus we speculate that the constituents of the mesophase in the drawn iPP fiber also contain oriented bundles of polymer chains, which have only partial packing ordering. As far as helical hands are concerned, the bundle consists of a statistical aggregation of chains with either a right- or a left-helical hand. We should mention that the mesophase formed during the fiber drawing process might have different superstructures when compared with those formed by quenching the material from the melt state. One researcher in our group found that there was a long period in the quenched iPP samples, although it was relatively weak. This finding was also confirmed by some previous studies [30, 31].

4. Conclusions

A new image analysis method was introduced to extract quantitative fractions of the crystal phase, amorphous phase and mesophase from 2D WAXD fiber patterns. The results showed that the average percentage of the mesophase in the Kevlar 49 aramid fiber was about 20 wt%. The mesophase may represent the highly oriented fraction of the chains with lattice registrations too poor to be considered as crystalline. It was found that the conversions between the crystal phase, mesophase and amorphous phase were small during deformation of Kevlar 49 fibers at room temperature. The SAXS pattern indicated that the superstructure of the Kevlar 49 fiber was mainly a fibrillar structure. 2D WAXD results of iPP fiber showed that the α-form crystallites were quite defective in the initial iPP fibers and were converted into the mesomorphic modification by drawing at room temperatures. The 1D equatorial peaks of the mesophase in both iPP and Kevlar 49 fibers showed a very similar broad peak, suggesting that they could have a similar nature. Corresponding 2D SAXS patterns of the mesophase in iPP fiber showed the shape of streak on the equator, instead of an obvious long period (i.e. no lamellar structure). We speculate that the constituents of the mesophase in the drawn iPP fibers may be oriented bundles of helical chains with random assembly of helical hands and perhaps also oriented chains without helical structures, due to the stereo/tacticity defects in contrast to the Kevlar 49, which has oriented chains without helical structures.

Acknowledgement

The authors thank Mr. Richard Hilmer for his assistance in developing the image analysis software. BC and BH are grateful for the financial support of this work by grants from the U.S. Army Research Office (DAAG559710022) and the U.S. Department of Energy (DEFG 0299 ER45760).

References

1. R. ANDROSCH, J. BLACKWELL, S. N. CHVALUN and B. WUNDERLICH, *Macromolecules* **32**(11) (1999) 3735.
2. R. ANDROSCH and B. WUNDERLICH, in Proc. Conf. North Am. Therm. Anal. Soc. 26th (1998) p. 469.
3. B. WUNDERLICH, *Macromol. Symp.* **113** (1997) 51.
4. G. NATTA, M. PERALDO and P. CORRADINI, *Rend. Accad. Naz. Lincei* **26** (1959) 14.
5. S. BRUCKNER, S. V. MEILLE, V. PETRACCONE and B. PIROZZI, *Prog. Polym. Sci.* **16** (1991) 361.
6. P. CORRADINI, C. DEROSA, G. GUERRA and V. PETRACCONE, *Polym. Comm.* **30** (1989) 281.
7. R. A. PHILLIPS and M. D. WOLKOWICZ, in "Polypropylene Handbook," edited by P. Edward Jr. Moore (Hanser Publishers, Munich, 1996) p. 419.
8. B. WUNDERLICH and J. GREBOWICZ, *J. Adv. Polym Sci.* **60/61** (1984) 1.
9. J. GREBOWICZ, J. F. LAU and B. WUNDERLICH, *J. Polym. Sci., Polym. Symp.* **71** (1984) 19.
10. P. CORRADINI, V. PETRACCONE, C. DEROSA and G. GUERRA, *Macromolecules* **19** (1986) 2699.
11. H. H. YANG, "Kevlar Aramid Fiber" (John Wiley & Sons Ltd. Chichester, England, 1993) p. 200.
12. M. G. DOBB, D. J. JOHNSON and B. P. SAVILLE, *J. Polym. Sci., Polym. Symp.* **58** (1977) 237.
13. D. J. SCHAEFER, R. J. SCHADT, K. H. GARDNER, V. GABARA, S. R. ALLEN and A. D. ENGLISH, *Macromolecules* **28** (1995) 1152.
14. R. J. SCHADT, E. J. CAIN, K. H. GARDNER, V. GABARA, S. R. ALLEN and A. D. ENGLISH, *ibid.* **26** (1993) 6503.
15. R. J. SCHADT, K. H. GARDNER, V. GABARA, S. R. ALLEN, D. B. CHASE and A. D. ENGLISH, *ibid.* **26** (1993) 6509.
16. C. L. JACKSON, R. J. SCHADT, K. H. GARDNER, D. B. CHASE, S. R. ALLEN, V. GABARA and A. D. ENGLISH, *Polymer* **35**(6) (1994) 1123.
17. B. CHU, P. J. HARNEY, Y. LI, K. LINLIU, F. YEH and B. S. HSIAO, *Rev. Sci. Instrum.* **65**(3) (1994) 597.
18. B. S. HSIAO, B. CHU, P. HARNEY, A. D. KENNEDY and R. A. LEACH, *J. Appl. Cryst.* **30** (1997) 1084.
19. S. RAN, D. FANG, X. ZONG, B. S. HSIAO, B. CHU and P. M. CUNNIFF, *Polymer* **42** (2001) 1601.
20. M. PANAR, P. AVAKIAN, R. C. BLUME, K. H. GARDNER, T. D. GIERKE and H. H. YANG, *J. Polym. Sci., Polym. Phys. Ed.* **21** (1983) 1955.
21. C. O. PRUNEDA, W. J. STEELE, R. P. KERSHAW and R. J. MORGAN, *Polym. Prepr. ACS Div. Polym. Chem.* **22** (1981) 216.
22. D. T. GRUBB, K. PRASAD and W. ADAMS, *Polymer* **32**(7) (1991) 1167.
23. S. RAN, X. ZONG, D. FANG, S. B. HSIAO, B. CHU and R. ROSS, *Journal of Applied Crystallography* **33** (2000) 1031.
24. F. DE CANDIA, P. IANNELLI, G. STAULO and V. VITTORIA, *Colloid & Polym. Sci.* **266**(7) (1988) 608.
25. R. SARAF and R. S. PORTER, *Mol. Cryst. Liq. Cryst. Letters* **2**(3, 4) (1985) 85.
26. H. W. WYCKOFF, *J. Polym. Sci.* **62** (1962) 83.
27. R. L. MILLER, *Polymer* **1** (1960) 135.
28. M. A. GOMEZ, H. TANAKA and E. TONELLI, *ibid.* **28** (1987) 2227.
29. A. MARTORANA, S. PICCAROLO and F. SCICHILONE, *Macromol. Chem. Phys.* **198** (1997) 597.
30. D. M. GEZOVICH and P. H. GEIL, *Polym. Eng. Sci.* **8** (1968) 202.
31. C. C. HSU, P. H. GEIL, H. MIYAJI and K. ASAI, *J. Polym. Sci., Polym. Phys. Ed.* **24** (1986) 2379.

Received 7 July
and accepted 23 November 2000